EBioMedicine 59 (2020) 102867

Contents lists available at ScienceDirect

EBioMedicine

journal homepage: www.elsevier.com/locate/ebiom

Research paper

Targeting a bacterial DNABII protein with a chimeric peptide immunogen or humanised monoclonal antibody to prevent or treat recalcitrant biofilm-mediated infections

Laura A. Novotny[a], Steven D. Goodman[a,b], Lauren O. Bakaletz[a,b,*]

[a] Center for Microbial Pathogenesis, Abigail Wexner Research Institute at Nationwide Children's Hospital, 700 Children's Drive, W591, Columbus, OH 43205 USA
[b] The Ohio State University College of Medicine, 700 Children's Drive, Columbus, OH 43210 USA

ARTICLE INFO

Article History:
Received 16 April 2020
Revised 2 June 2020
Accepted 15 June 2020
Available online 7 July 2020

Keywords:
Fabs
Integration host factor
Tip-chimeric peptide
Otitis media
Therapeutic
Preventative

ABSTRACT

Background:: Chronic and recurrent bacterial diseases are recalcitrant to treatment due to the ability of the causative agents to establish biofilms, thus development of means to prevent or resolve these structures are greatly needed. Our approach targets the DNABII family of bacterial DNA-binding proteins, which serve as critical structural components within the extracellular DNA scaffold of biofilms formed by all bacterial species tested to date. DNABII-directed antibodies rapidly disrupt biofilms and release the resident bacteria which promote their subsequent clearance by either host immune effectors or antibiotics that are now effective at a notably reduced concentration.

Methods:: First, as a therapeutic approach, we used intact IgG or Fab fragments against a chimeric peptide immunogen designed to target protective epitopes within the DNA-binding tip domains of integration host factor to disrupt established biofilms *in vitro* and to mediate resolution of existing disease *in vivo*. Second, we performed preventative active immunisation with the chimeric peptide to induce the formation of antibody that blocks biofilm formation and disease development in a model of viral-bacterial superinfection. Further, toward the path for clinical use, we humanised a monoclonal antibody against the chimeric peptide immunogen, then characterised and validated that it maintained therapeutic efficacy.

Findings:: We demonstrated efficacy of each approach in two well-established pre-clinical models of otitis media induced by the prevalent respiratory tract pathogen nontypeable *Haemophilus influenzae*, a common biofilm disease.

Interpretation:: Collectively, our data revealed two approaches with substantive efficacy and potential for broad application to combat diseases with a biofilm component.

Funding: Supported by R01 DC011818 to LOB and SDG.

1. Introduction

There is a substantial health and economic burden presented by chronic and recurrent diseases of the airways, urogenital tract, skin and oral cavity, and up to 80% of these include bacterial biofilms [1,2]. Often multispecies in composition, biofilms (adhered to a surface or as aggregates) readily form on or within abiotic and biotic surfaces [2–4] in response to environmental cues and stresses and thus promote bacterial survival. Once established, the resident bacteria self-produce, and become encased in, extrapolymeric substances (EPS), which serve to protect the resident cells from unfavorable environmental conditions or assault by host immune effectors [5]. In concert with the altered/reduced metabolism of biofilm-resident bacteria, the EPS also protects against the action of antibiotics, with concentrations of >1000-fold greater than a standard therapeutic dose required to achieve killing similar to that of planktonic bacteria [6–8]. As such, novel means to disperse or disrupt biofilms are required [5,9,10] and ideally, one would also develop methods to prevent their formation.

Toward a therapeutic approach for biofilm disruption, our laboratory has shown that incubation of bacterial biofilms with antibody directed against either of the two members of the DNABII family of bacterial DNA-binding proteins, integration host factor (IHF) or the histone-like protein (HU), induces collapse due to their role as linchpin proteins positioned at the vertices of crossed strands of extracellular DNA (eDNA) which form a lattice, and thereby provides

* Corresponding author at: Center for Microbial Pathogenesis, Abigail Wexner Research Institute at Nationwide Children's Hospital, 700 Children's Drive, W591, Columbus, OH 43205 USA.
E-mail address: Lauren.Bakaletz@nationwidechildrens.org (L.O. Bakaletz).

https://doi.org/10.1016/j.ebiom.2020.102867

Research In Context

Evidence before this study

The enduring symptomatic or intermittently (cyclical) symptomatic nature of many chronic, and recurrent bacterial diseases, respectively is largely attributable to the presence of a biofilm. An abundant component of the biofilm is bacterial extracellular DNA (eDNA), arranged in a lattice, the structure of which is maintained by the DNABII family of bacterial DNA-binding proteins. There are only two members of the DNABII family: integration host factor (IHF) and histone-like protein (HU). Both proteins are critical components of the matrix formed by all human pathogens tested to date. Within a biofilm, IHF binds to eDNA of the biofilm via its DNA-binding 'tip' regions, and thus the amino terminal ('tail') region is exposed. Antibody directed to tail region does not disrupt biofilms, however antibody that targets the eDNA-occluded tip regions of IHF induces significant biofilm collapse. Development of a chimeric peptide immunogen to induce antibody that specifically targets the protective tip regions of both subunits of IHF effectively disrupts nontypeable *Haemophilus influenzae* (NTHI) biofilms *in vitro* and mediates either rapid resolution or prevention of disease in two pre-clinical models of otitis media (OM).

Added value of this study

The aims of this study were to 1) test the pre-clinical therapeutic potential of the antigen binding domains of IgG (Fab fragments) of a monoclonal antibody directed against a DNABII-directed tip-chimeric peptide to resolve a well-characterised biofilm disease, OM due to NTHI, and 2) test this same tip-chimeric peptide as an immunogen for its ability to induce antibodies that would prevent biofilm formation and disease when used as a vaccine antigen in active immunisation regimens as a complementary preventative strategy. We first established that Fabs- or intact IgG against the tip-chimeric peptide mediated disruption of bacterial biofilms *in vitro*. We then used two well-established chinchilla models of OM due to NTHI (one based on direct bacterial challenge of the middle ear and the other, a viral-bacterial superinfection model of ascending OM) and demonstrated the pre-clinical efficacy of both our DNABII-directed therapeutic and prevention strategies, respectively. Lastly, we humanised one DNABII-directed monoclonal antibody and validated its activity *in vitro* as well as its therapeutic efficacy pre-clinically.

Implication of all the available evidence

We now present a refined two-pronged approach against bacterial biofilms, both of which target the eDNA+DNABII scaffold of the bacterial biofilm. The first is a therapeutic strategy wherein IgG or Fab fragments of antibodies directed against the tip-chimeric peptide immunogen (and ultimately, a humanised monoclonal antibody), are delivered directly into the middle ear to disrupt established NTHI biofilms and mediate resolution of experimental OM. The second approach is a preventative active immunisation strategy wherein the tip-chimeric peptide is used as an immunogen to induce the formation of antibody that blocks biofilm formation by NTHI in the middle ear and thereby, development of experimental OM.

structural support to the biofilm [11]. This outcome is rapid and specific and does not require direct contact of antibody with the biofilm [12,13]. The mechanism for biofilm disruption is due to sequestration of any free DNABII proteins from the milieu that surrounds the biofilm, which induces a shift in equilibrium such that DNABII proteins bound to the biofilm's eDNA-rich structural lattice are driven into the released state [12,14]. The outcome is significant destabilisation of the eDNA+DNABII protein matrix and subsequent collapse of the biofilm structure [12]. Previous biofilm-resident bacteria are thus released from their protective matrix and now subject to clearance by host immune effectors or antibiotics. Notably, these newly released bacteria are exquisitely more sensitive to the action of antibiotics, such that concentrations 4–8-fold less that those required to kill their planktonic counterparts are now equally effective [12,15].

Our DNABII antibody-mediated biofilm disruption approach is species-independent as we have shown it to be broadly effective against all 22 bacterial species tested thus far *in vitro*, the panel of which includes Gram-positive and Gram-negative species and the high priority ESKAPE pathogens (*Enterococcus faecium, Staphylococcus aureus, Klebsiella pneumoniae, Acinetobacter baumannii, Pseudomonas aeruginosa* and *Enterobacter* spp.) [16–23]. DNABII-directed antibodies will also disrupt polymicrobial biofilm fragments (*e.g.* eDNA+DNABII protein lattices) within clinical specimens recovered from patients with post-tympanostomy tube otorrhea [24], cystic fibrosis[19] and Cesarean section wound infections [23]. Moreover, this approach is proven to be significantly effective pre-clinically in three experimental models of chronic human diseases: otitis media (OM) induced by nontypeable *Haemophilus influenzae* (NTHI) in the chinchilla [13,21], lung infection due to *Pseudomonas aeruginosa* in the murine host [21] and in a rat model of *Aggregatibacter actinomycetemcomitans*-induced periodontal peri-implantitis [18].

As we show significant therapeutic efficacy with antibodies against DNABII proteins pre-clinically, several questions nonetheless remained to be addressed on our path toward clinical use. First, whereas we have shown that anti-DNABII antibodies are highly effective to disrupt bacterial biofilms, we wondered whether Fab fragments alone would also mediate equivalent collapse of the biofilm structure and thereby could serve as an alternate therapeutic to use of intact IgG against diseases with a biofilm component, particularly when repeated dosing might be required, in order to prevent formation of anti-antibodies [1]. Second, given that IHF exists as a heterodimer of IHFA and IHFB subunits [25], we asked whether an approach that targets immunoprotective domains within both subunits simultaneously might be more effective than our previous approach which targeted only a single subunit. As such, we designed an epitope-targeted synthetic chimeric peptide and tested the relative efficacy of Fab fragments of a monoclonal antibody directed against it for use as a potential therapeutic agent against a well-characterised biofilm disease. Third, whereas development of therapeutic antibodies is a rational approach to resolve bacterial biofilms, we also pursued the complementary preventative strategy wherein this same chimeric peptide immunogen was tested for its ability to prevent biofilm formation and disease when used as a vaccine antigen in active immunisation regimens. Herein, we addressed these unknowns.

2. Materials and methods

2.1. Murine monoclonal antibodies, polyclonal rabbit antibodies and humanised monoclonal antibodies

Murine monoclonal antibodies against β-tip (clone 12E6.F8.D12.D5, mIhfB4$_{NTHI}$) or β-tail (clone 7A4.E4.G11, IhfB2$_{NTHI}$) domains of IHF$_{NTHI}$ were purified from cell culture supernatants as previously described [21]. Mouse IgG1κ isotype control antibody (clone P3.6.2.8.1; eBioscience cat# 16-4714-82, RRID: AB_470161) served as a negative control. Fab fragments were then generated by papain digestion with Mouse IgG1 Fab and F(ab')2 preparation kit (Pierce) according to instructions. Polyclonal rabbit anti-tip chimeric peptide and anti-tail chimeric peptide were generated at Rockland Immunochemical, Inc [13]. Naive rabbit serum served as a negative control. IgG was enriched from each rabbit serum by passage through rProtein A Protein G GraviTrap columns (GE Healthcare) according to manufacturer's instructions. Fab fragments (Fabs) were then

generated via Pierce Fab Preparation kit. Digestion of intact murine or rabbit IgG to Fabs was confirmed by SDS-PAGE with Coomassie Fluor™ Orange Protein Gel stain (ThermoFisher). Humanised monoclonal antibodies against the tip chimeric peptide (HuTipMab) or tail chimeric peptide (HuTailMab) were generated at LakePharma, Inc. The antigen-binding domains were derived from a murine monoclonal antibody directed against the tip chimeric peptide (clone 1F8.C3.D11.F1) or tail chimeric peptide (clone 11E7.G11.C7). Humanised monoclonal antibody clones TP-21949 (tip chimeric peptide-directed; HuTipMab) and TP-21958 (tail chimeric peptide-directed; HuTailMab) were used for the work herein. Bacterial endotoxin test via ToxinSensor Chromogenic LAL endotoxin kit (Genscript) was performed on all antibody lots prior to use.

2.2. In vitro *biofilm disruption*

Biofilms formed by NTHI strain 86−028NP (a minimally passaged clinical isolate from the nasopharynx of a child with chronic OM) [26], *Moraxella catarrhalis* strain 7169 (a minimally passaged clinical isolate from the middle ear of a child with chronic OM) [27], *P. aeruginosa* strain 27853 (ATCC), *Burkholderia cenocepacia* strain K56 (isolated from the sputum of a patient with cystic fibrosis)[28] and *S. aureus* strain 29213 (ATCC) were first established in 8-well chambered coverglass (CellVis) for 24 h prior to incubation with 170 nM intact IgG or Fab fragments for an additional 16 h [11,29]. A concentration of 170 nM was based on prior studies wherein 5 μg intact IgG per 0.2 ml volume was applied to *in vitro* biofilms [11−13,20,21] to permit direct comparison between IgG- *versus* Fabs-mediated disruption. Bacteria within the biofilms were then stained with FM1−43FX (ThermoFisher), fixed overnight in a solution of 16% paraformaldehyde- 4% acetic acid- 2.5% glutaraldehyde in 0.1 M phosphate buffer (pH 7.4) then washed with 10 mM phosphate-buffered saline (pH 7.4). Biofilms were viewed with a Zeiss 800 scanning confocal laser microscope, images rendered in Zeiss Zen Pro-software and biomass determined with COMSTAT2 software [30]. *In vitro* biofilm disruption assays were repeated three times on separate days.

2.3. *Animals*

Chinchilla work was performed in accordance with the NIH Guide for the Care and Use of Laboratory Animals and under protocol #01304AR approved by Abigail Wexner Research Institute at Nationwide Children's Hospital Animal Care and Use Committee. Juvenile or adult chinchillas (*Chinchilla lanigera;* juvenile animals were 250−499 g in body mass; adult animals were 500−850 g in body mass) were obtained from Rauscher's Chinchilla Ranch, LLC. These outbred, non-specific pathogen-free animals were housed in individual cages with autoclaved corncob bedding and sterile water provided *ad libitum*. Animals were randomly divided into cohorts based on body weight (as an indication of juvenile or adult status) and both male and female animals were used. Experimental groups were as follows: to examine disruption of NTHI biofilms from the middle ear as induced by murine β-tip Fabs, β-tail Fabs or isotype control Fabs, three or four animals were enrolled into each cohort (mean body mass per cohort, 625 g). To test biofilm disruption induced by Fabs from rabbit polyclonal anti-tip chimeric peptide serum IgG, anti-tail chimeric peptide serum IgG or IgG from naive rabbit serum, cohorts of three chinchillas each were established (mean body mass per cohort, 505 g). Efficacy of HuTipMab, compared to HuTailMab or saline was evaluated with three animals per cohort (mean body mass per cohort, 580 g). To evaluate the ability of the tip chimeric peptide to induce production of antibodies that prevented the development of NTHI-induced OM, eight juvenile animals were used per cohort (mean body mass per cohort, 430 g).

2.4. *Disruption of NTHI biofilms formed in the middle ears of chinchillas in experimental OM*

Both middle ears of each animal were challenged with 1000 CFU NTHI strain 86-028NP by direct injection to induce experimental OM. Four days later, NTHI mucosal biofilms fill >50% of the middle ear [31]. At this time, 342 nM Fabs or humanised monoclonal antibody was injected into each middle ear (0.1 ml delivered per bulla), with identical treatment delivered 24 h later. A concentration of 342 nM was based on prior studies wherein 5 μg intact IgG per 0.1 ml volume was injected into the middle ears of chinchillas [11,13,21] and to permit direct comparison between IgG- *versus* Fabs-mediated disruption *in vivo*. To determine the immediate outcome of treatment, animals were sacrificed one day after completion of antibody therapy, images of mucosal biofilms captured with a Zeiss SV6 dissecting microscope, then mucosal biofilms and middle ear mucosa collected, homogenised and plated on to chocolate agar to semi-quantitate the non-planktonic bacterial load within the middle ear [11]. In two of the studies described herein (assessment of biofilms disruption by polyclonal rabbit IgG Fab fragments and efficacy of humanised monoclonal antibody to disrupt mucosal biofilms), a subset of animals in each cohort was monitored an extra seven days without additional treatment to examine whether NTHI biofilms would re-form upon cessation of antibody therapy. Mucosal biofilms were collected and processed as described [11].

2.5. *Qualitative assessment of amount of mucosal biofilm*

As an additional assessment, the amount of biofilm in each middle ear was qualitatively determined. Images of each middle ear were captured, randomised and ranked by six reviewers blinded to treatment delivered using an established rubric wherein 0= no mucosal biofilm visible, 1= <25% of middle ear occluded by mucosal biofilm, 2= ≥25-<50% occluded, 3= ≥50- <75% occluded, 4= ≥75−100% occluded [31]. For both quantitation of bacterial load and qualitative assessment of mucosal biofilm, each middle ear was considered independent.

2.6. *Quantitation of cytokines in middle ear fluids*

To quantitate cytokines in middle ear fluids (MEF) a BD™ Cytometric Bead Array was performed with fluids collected at the time of animal sacrifice. With BD™ human-specific Flex Sets each MEF was individually examined for quantity of IL-1β (cat# 558279), IL-6 (cat# 558276), IL-8 (cat# 558277), IL-10 (cat# 558274), IL12-p70 (cat# 558283), IL-17A (cat# 560383) and TNF (cat# 560112) using according to manufacturer's instructions. The cytokine IL-13 (cat# 558450) was added to the panel used to assay MEF collected in the HuMabs study. MEF from each animal were assayed individually. Data were captured on a BD Accuri™ C6 cytometer (BD Biosciences) and analysed with FlowJo software (FlowJo, LLC). The concentration of cytokines in each MEF was determined using a standard curve and calculated using GraphPad Prism software.

2.7. *Surface plasmon resonance*

To determine the affinity of the humanised tip chimeric peptide-directed monoclonal antibody to the tip chimeric peptide and to native IHF_{NTHI}, surface plasmon resonance using a Biacore 3000 instrument (GE Healthcare Life Sciences) was performed. All experiments were conducted at 25 °C and 10 mM HEPES (pH 7.4)- 150 mM NaCl- 3 mM EDTA- 0.005% Surfactant P20 (HBS-EP; GE Healthcare, cat# BR100188) served as the running buffer. Via amine couple chemistry and at a flow rate of 5 μl/ min, HuTipMab was immobilised to flow cells of a CM5 sensor chip (GE Healthcare, cat# BR100012) to 4000 resonance units (RU) to assay binding of tip chimeric peptide or 2000 RU to assess binding of native IHF_{NTHI}. Next, tip chimeric

peptide or native IHF_{NTHI} was suspended in HBS-EP plus NSB reducer (GE Healthcare, cat# BR100691) and serial two-fold dilutions from 100 nM to 3.1 nM, including a buffer-only sample, were injected across the antibody-bound surface at a flow rate of 30 μl/ min, 5 min injection time, 5 min dissociation time using the KINJECT command. BiaEvaluation software (GE Healthcare) was used to align sensorgram curves, subtract buffer-only injection cycle and determine K_D values.

2.8. Viral-bacterial co-infection model of experimental NTHI-induced OM

An established adenovirus-NTHI polymicrobial challenge model [32] was employed to assess efficacy of the tip chimeric peptide when delivered as a pre-clinical vaccine antigen. Chinchillas were randomly divided into three cohorts of eight animals each based on body weight and immunised by rubbing vaccine formulations on to the unabraded skin behind each pinna (post-auricular region) [33]. Formulations consisted of 10 μg tip chimeric peptide or 10 μg tail chimeric peptide, each admixed with 10 μg of the adjuvant LT (R192G/L211A), a double mutant of *E. coli* heat labile enterotoxin (dmLT; a generous gift from Dr. John D. Clements, Professor Emeritus, Tulane University School of Medicine) [34]. As a negative control, one cohort received 10 μg dmLT only. A second identical dose was delivered one week later. Two days after receipt of the second dose, the time when the maximal immune response is observed for this immunisation regimen [35], all chinchillas were inoculated with 1.9×10^7 $TCID_{50}$ of adenovirus serotype 1 by passive inhalation of droplets. Seven days later, when adenovirus-induced compromise of the airway occurs [32], all animals were challenged with 10^8 CFU NTHI strain 86-028NP by passive droplet inhalation. To confirm that all cohorts were equivalently colonised by NTHI (now resident within the nasopharynx) and thereby available to ascend the virus-compromised Eustachian tube, a nasopharyngeal lavage was performed one day after bacterial challenge. Nasopharyngeal lavage fluids were serially diluted and plated on to chocolate agar plus 15 μg ampicillin/ml medium to limit growth of normal chinchilla flora (this concentration of ampicillin has no effect on growth of NTHI strain 86-028NP) [33]. NTHI colonies were enumerated after incubation for 24 h at 37 °C.

2.9. Video otoscopy

Video otoscopy was performed on all animals using a Welch Allyn MacroView™ otoscope and Welch Allyn Viewer software. Each tympanic membrane was blindly ranked on an established scale of 0 to 4, and middle ears with a score of $\geq$2.0 were considered positive for OM as inflammation (erythema) and MEF were visible [36]. If one middle ear was ranked $\geq$2.0, but the contralateral ear was ranked $<$2.0, the animal was considered positive for OM. To calculate vaccine efficacy, the number of observations of OM during the 20-day study period was first determined and converted to a percentage relative to the total number of observations for each cohort. This value was then subtracted from the percentage computed for the cohort given dmLT only. Video otoscopy was performed by an individual blinded to formulation delivered.

2.10. Statistical analyses

Graphical results and statistical tests were performed with GraphPad Prism 8. Differences in biomass for *in vitro* biofilm disruption assays were determined by one-way ANOVA with multiple comparisons. Differences in quantity of cytokines in middle ear fluids among cohorts was determined by determined by one-way ANOVA with multiple comparisons. Differences in bacterial load and mean mucosal biomass score were determined by one-way ANOVA with multiple comparisons. Delay to onset of OM and time to resolution of disease was determined by Mantel-Cox test.

2.11. Role of the funding source

No funding source was involved in study design, or conduct, analysis and interpretation of data, in the writing of the manuscript, or in the decision to submit the paper for publication.

2.12. Availability of biological materials

Biological materials will be made available upon request solely for internal, non-commercial research purposes and with the requirement that reasonable costs of distribution are provided.

3. Results

3.1. β-tip Fab fragments from a murine monoclonal antibody disrupted bacterial biofilms in vitro

Before the conduct of *in vivo* studies, we first performed an *in vitro* chambered coverglass assay wherein biofilms formed by five diverse bacterial species were allowed to form for 24 h prior to incubation with Fab fragments to validate their potential activity. Fab fragments were derived from a murine monoclonal antibody directed against a 15-mer previously-defined immunoprotective domain within the DNA-binding 'tip' region of the β-subunit of NTHI IHF (IHF_{NTHI}), herein referred to as 'β-tip Fabs' [12], and compared the outcome to that induced by use of the respective intact IgG molecule. As negative controls, Fab fragments derived from a murine monoclonal antibody against a 15-mer non-protective domain within the 'tail' region of the β-subunit of IHF_{NTHI} ('β-tail Fabs'), which does not disrupt bacterial biofilms [21] or nonspecific murine IgG1 isotype antibody ('isotype control Fabs') were used.

Representative images revealed that each of the five diverse bacterial species tested formed biofilms of varied architecture within 24 h [Fig. 1a]. β-tail Fabs or isotype control Fabs had no disruptive effect, similar to the outcome with intact IgG from which these negative control fragments were derived. In contrast, incubation with β-tip Fabs was significantly disruptive of the biofilms formed by all bacterial species tested. Quantitation of biofilm biomass revealed that biofilm disruption by this concentration of β-tip Fabs was comparable to that achieved with an equimolar concentration of the respective intact β-tip IgG ($P \leq 0.05$; one-way ANOVA with multiple comparisons) [Fig. 1b]. Thus, the minimal antigen-binding domain of the β-tip-directed antibody molecule was sufficient to bind to, and sequester DNABII protein, then disrupt the biofilm as effectively as the intact antibody from which the Fab fragments were generated.

3.2. Murine β-tip Fabs eradicated NTHI from biofilms and resolved biofilms during experimental OM

With biofilm-disruptive function of the β-tip Fabs now demonstrated *in vitro*, we were able to address our first question: in the context of experimental disease, is antibody-mediated DNABII protein sequestration via only the Fab domains sufficient to induce biofilm collapse with subsequent clearance of released bacteria? To answer this query, we employed a well-established chinchilla model of OM due to the predominant pathogen of chronic and recurrent disease, NTHI. Experimental OM was first induced by direct challenge of the middle ear. After four days, NTHI biofilms fill the middle ear [31]. Murine monoclonal antibody-derived β-tip Fabs, β-tail Fabs or isotype control Fabs were then injected into both middle ears, with a second identical treatment given 24 h later [Fig. 2a]. One day after receipt of the second dose of Fabs, all animals were sacrificed to assess relative immediate treatment efficacy.

We first quantitated the number of NTHI resident within mucosal biofilms and/or adherent to the middle ear mucosa by plate count. There was no difference in the bacterial load in animals that received

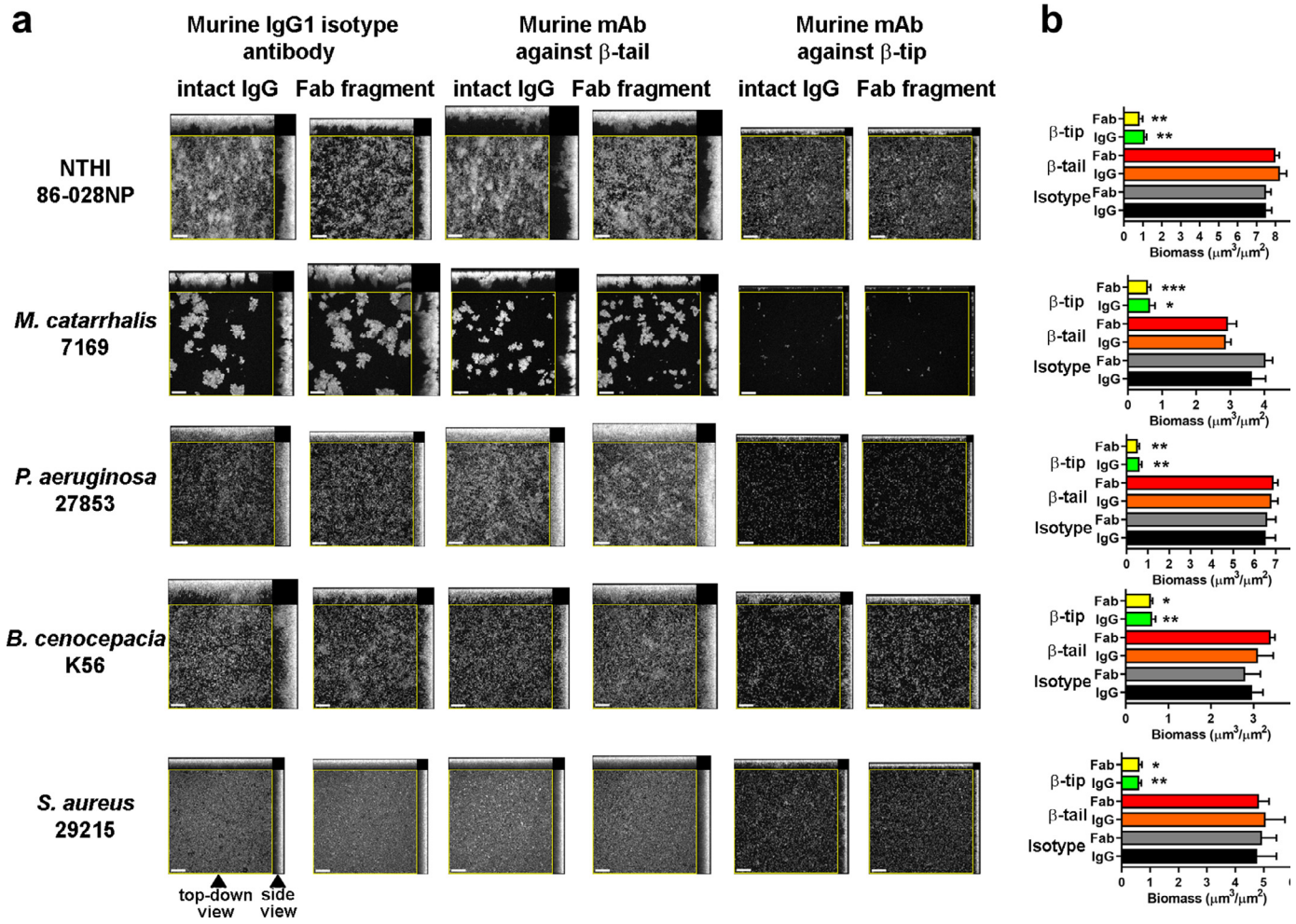

Fig. 1. Murine monoclonal antibody-derived Fab fragments disrupted biofilms formed by five human pathogens *in vitro*. (a) Representative images of bacterial biofilms (pseudocoloured white) revealed significant biofilm disruption by 170 nM intact IgG or Fabs directed against the β-tip domain of IHF. Orthogonal projections show a top-down view to depict spatial distribution of biofilm in x-y plane and side view indicates biofilm height in z-plane (arrowheads). Scale bars, 20 μm. (b) Biomass within each image as quantitated by COMSTAT2 software. Each assay was repeated three times on different days and the mean ± SEM shown. $^{*}P \leq 0.05$, $^{**}P \leq 0.01$ compared to respective intact IgG or Fabs [one-way ANOVA with multiple comparisons].

β-tail Fabs compared to isotype control Fabs [Fig. 2b]. Conversely, a significant 4-log fewer NTHI were detected within mucosal biofilms recovered from animals treated with β-tip Fabs and in one of the six middle ears in this cohort, all NTHI had been eradicated ($P \leq 0.01$; one-way ANOVA with multiple comparisons) [Fig. 2b]. Thus, delivery of β-tip Fabs induced augmented eradication of NTHI from chinchilla middle ears.

To next discern whether any of the three treatments induced rapid resolution of the established NTHI biofilms, one day after completion of Fab fragment therapy images of each middle ear were captured, randomised and ranked by six blinded reviewers. Reviewers used an established rubric wherein a score of 0 equated to no mucosal biofilm observed, and a score of 4+ indicated that ≥75% of the middle ear remained filled with mucosal biofilm. Accordingly, β-tail Fabs induced a slight but nonsignificant reduction in amount of mucosal biofilm when compared to delivery of isotype control Fab fragments. Importantly, ≥50% of the middle ears in the isotype control Fab and β-tail Fabs cohorts remained filled with mucosal biofilm with mean biomass scores of 3.4 and 2.7, respectively [Fig. 2c]. Conversely, β-tip Fabs induced a significant reduction in mucosal biofilm ($P \leq 0.05$; one-way ANOVA with multiple comparisons) and a majority (4 of 6, 67%) of middle ears in this latter cohort were assigned a score ≤1.0 which indicated that ≤25% of the middle ear contained any residual visible biofilm. Thus, delivery of β-tip Fabs both significantly reduced the bacterial load in the middle ears and induced effective eradication of already established mucosal biofilms.

Representative images of a middle ear from each cohort are presented in Fig. 2d with both a healthy chinchilla middle ear and one filled with an NTHI biofilm shown for reference. In naive animals, the middle ear mucosa and full length of the natural bony septae are visible (score 0). In contrast, four days after NTHI challenge, neither the thin mucosal lining of the middle ear nor the bony septae are visible as these anatomical features are now occluded by a large mucosal biofilm (score 4). In this study, after delivery of β-tail Fabs or isotype control Fabs, mucosal biofilms still filled 50−100% of the middle ears, with a representative assigned score of 4.0 or 2.4, respectively [Fig. 2d]. However, β-tip Fabs largely eradicated these structures as evidenced by the fact that both the middle ear mucosal lining and the bony septae were fully visible (assigned score of 1.0). Also of note, whereas extensive inflammation was observed in the middle ear mucosae and tympanic membranes of animals that received β-tail Fabs (Fig. 2d, middle image, right side), there was only limited fine capillary dilatation within the middle ear mucosae of animals treated with β-tip Fabs (Fig. 2d, bottom image, right side) despite the fact that just two days earlier these ears were filled with a biofilm formed by NTHI.

To begin to understand why the middle ears of animals that received β-tail Fabs consistently appeared to be overtly inflamed

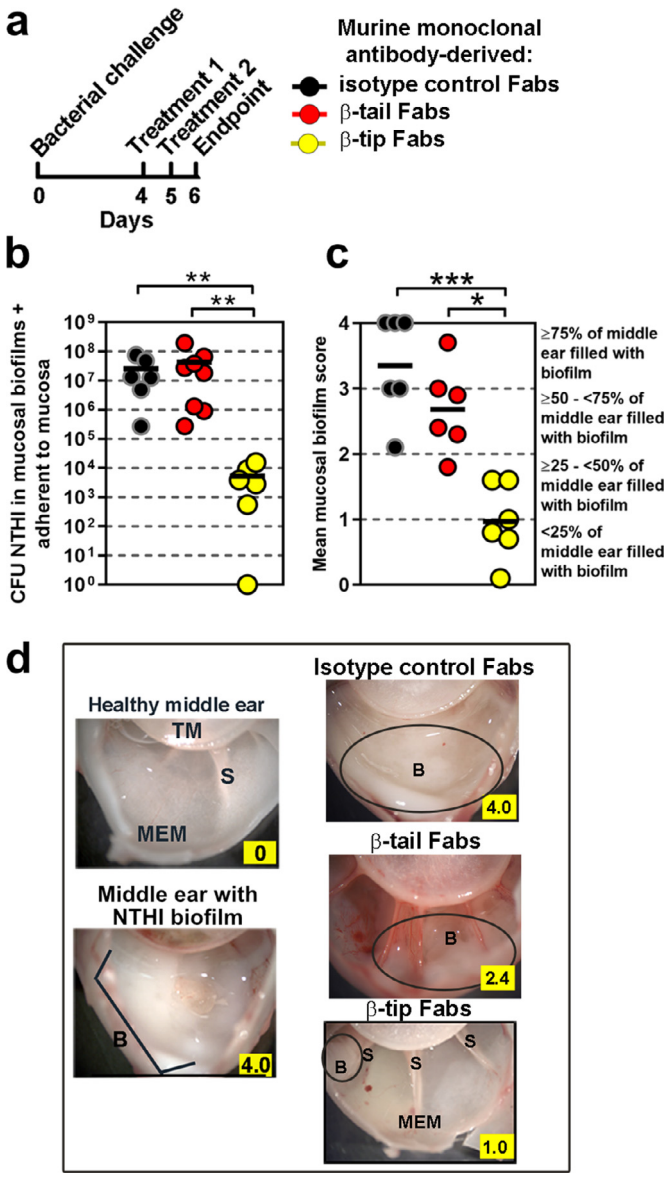

Fig. 2. Murine monoclonal antibody β-tip Fabs mediated eradication of biofilm-resident NTHI and resolution of mucosal biofilms from the middle ear. (a) Study timeline and treatments given. A dose of 342 nM Fabs was delivered into each middle ear. (b) Relative quantity of NTHI within mucosal biofilms and adherent to the middle ear mucosa amongst treated cohorts. (c) Relative mucosal biofilm score determined by six reviewers blinded to treatment amongst treated cohorts. Panels b & c: 6–8 middle ears per cohort, values for individual ears and mean for cohort shown. $^{*}P \leq 0.05$, $^{**}P \leq 0.01$, $^{***}P \leq 0.001$ [One-way ANOVA with multiple comparisons]. (d) Representative images of chinchilla middle ears from each cohort, mean mucosal biofilm score for the ear indicated within yellow box. TM, tympanic membrane; S, bony septae; MEM, middle ear mucosa; B, biofilm (encircled).

(Fig. 2d, middle image, right side), whereas β-tip Fabs-treated ears were not (Fig. 2d, bottom image, right side), we determined a focused cytokine profile within middle ear fluids collected from animals at the time of sacrifice. Via cytometric bead assay, a significantly greater quantity of each of a panel of six pro-inflammatory cytokines was detected in the middle ears of animals that received β-tail Fabs, compared to animals treated with β-tip Fabs ($P \leq 0.05$) [Fig. 3a]. Conversely, significantly more of the anti-inflammatory cytokine IL-10 was detected in middle ear fluids of animals that received β-tip Fabs ($P \leq 0.05$; one-way ANOVA with multiple comparisons) [Fig. 3b]. Moreover, compared to animals that received isotype control Fabs, significantly more of the pro-inflammatory cytokines IL-1β and TNF were detected in middle ear fluids from animals treated with β-tail Fabs [Fig. 3b], which likely contributed to the inflammation consistently observed within the mucosa in this cohort (see Fig. 2d, middle panel, right side). These data suggested that in the context of active experimental OM, biofilm collapse and clearance of NTHI induced by β-tip Fabs also mediated resolution of disease-associated inflammation.

Collectively, and central to our original question, to this point our data showed that β-tip Fabs effectively disrupted bacterial biofilms *in vivo,* thus the Fc portion of the anti-DNABII-directed antibody was not required to induce biofilm collapse. This result added support to our model wherein biofilm structural collapse, with release of resident bacteria, is the result of an DNABII protein targeted antibody-mediated equilibrium shift that subsequently tips the balance in favor of the host to now effectively eradicate newly released pathogens via engagement of multiple host immune effectors.

3.3. *Rabbit IgG Fabs against domains within both IHF subunits rapidly disrupted biofilms* in vivo

Thus far, we examined Fab fragments directed against the β-subunit, one of two heterologous subunits that comprise IHF_{NTHI}. While this approach was effective, in previous work we demonstrate that a cocktail of murine monoclonal antibodies against tip domains within the α-subunit plus those against the β-subunit of IHF_{NTHI} induces significantly greater biofilm disruption compared to antibody against either subunit individually, including those bacterial species that only possess an HU allele [21]. Although 74.7% similar in amino acid sequence, there is only 47.3% identity within each 94 amino acid subunit of IHF_{NTHI}, thus the cocktail of α-subunit- plus β-subunit-directed antibodies afforded broader coverage of the complete diversity within IHF and its orthologue, HU. With that information, we then designed an epitope-targeted, chimeric peptide immunogen to first induce antibody in a rabbit against both protective domains concurrently. Designated 'tip chimeric peptide', slightly larger (*e.g.* 20-mer) segments from within the DNA-binding tip domains of both the α-subunit and β-subunit of IHF_{NTHI} were incorporated and joined by a 4-residue linker peptide to permit flexibility between these two protective epitopes [13]. As a negative control, a 'tail chimeric peptide' immunogen was also developed that incorporated 20-mer segments from non-protective domains within the tail region of the α-subunit and β-subunit of IHF_{NTHI} and joined by the same 4-residue linker. We have previously shown that polyclonal rabbit IgG against this tip chimeric peptide disrupts biofilms formed by multiple bacterial species *in vitro* and resolves mucosal biofilms within the middle ears of chinchillas during experimental NTHI-induced OM [13].

To now merge our chimeric peptide design strategy with determination of potential Fab fragment-mediated therapeutic biofilm disruption, herein, we tested the ability of polyclonal rabbit anti-tip chimeric peptide Fabs to disrupt NTHI biofilms already present in the middle ear of chinchillas with experimental OM. We also evaluated the endurance of any resultant biofilm resolution, *i.e.* would NTHI biofilms re-establish once antibody therapy ceased? Accordingly, NTHI was allowed to establish large biofilms in the chinchilla middle ear before we delivered treatment with either Fabs derived from polyclonal rabbit IgG against: 1) tip chimeric peptide; 2) tail chimeric peptide or 3) naive serum [Fig. 4a]. One day after delivery of the second therapeutic dose, a subset of animals in each cohort was sacrificed to examine the immediate effect of treatment. The remaining animals were monitored an additional seven days, without further treatment, to assess the durability of this therapeutic approach.

One day after receiving two doses of tip chimeric peptide Fabs, there were >2-log fewer NTHI within mucosal biofilms and/or adherent to the middle ear mucosa, compared to either of the two negative control cohorts ($P \leq 0.05$; one-way ANOVA with multiple comparisons) [Fig. 4b]. After an additional week without further treatment, there was only a slight decrease in NTHI load within middle ear mucosal biofilms/adherent to the mucosa of animals given tail

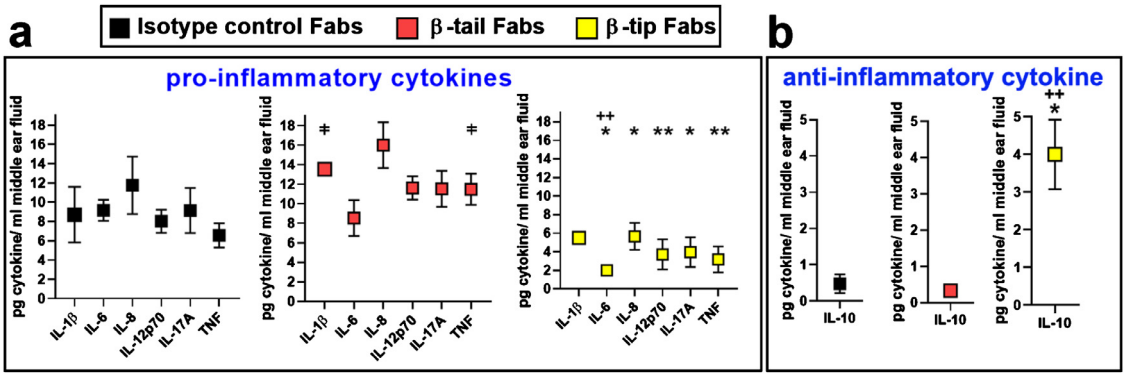

Fig. 3. Pro-inflammatory cytokines predominated in middle ear fluids from animals treated with 342 nM murine monoclonal antibody-derived β-tail Fabs. (a) Relative quantity of pro-inflammatory cytokines in chinchilla middle ear fluids after NTHI challenge and Fab fragment therapy as determined by cytometric bead array. $^{*}P \leq 0.05$, $^{**}P \leq 0.01$ *vs.* β-tip Fabs [one-way ANOVA with multiple comparisons], $\ddagger P \leq 0.05$ *vs.* isotype control Fabs [unpaired *t*-test]. (b) Relative mean concentration of the anti-inflammatory cytokine IL-10 amongst the three Fab fragment treated cohorts. $^{*}P \leq 0.05$ *vs.* β-tail Fabs, $^{++}P \leq 0.01$ *vs.* β-tail Fabs or isotype control Fabs [one-way ANOVA with multiple comparisons]. 5–7 middle ear fluids tested per cohort. Mean cytokine concentration ± SD shown.

chimeric peptide Fabs or naive serum Fabs. Conversely, at this latter time point, in animals given tip chimeric peptide Fabs there was an added 10-fold decrease in bacterial load ($P \leq 0.05$; one-way ANOVA with multiple comparisons). Notably, in 4 of 6 (67%) middle ears, these homogenised tissues were culture-negative for NTHI. These data suggested that NTHI released from the biofilm by tip chimeric peptide Fabs were subsequently cleared by host immune effectors without any additional intervention or treatment.

We next qualitatively evaluated whether treatment with these chimeric peptide-directed Fabs was able to eradicate NTHI biofilms already present in the chinchilla middle ear. To do so, blinded evaluators were asked to rank the relative amount of mucosal biofilm that

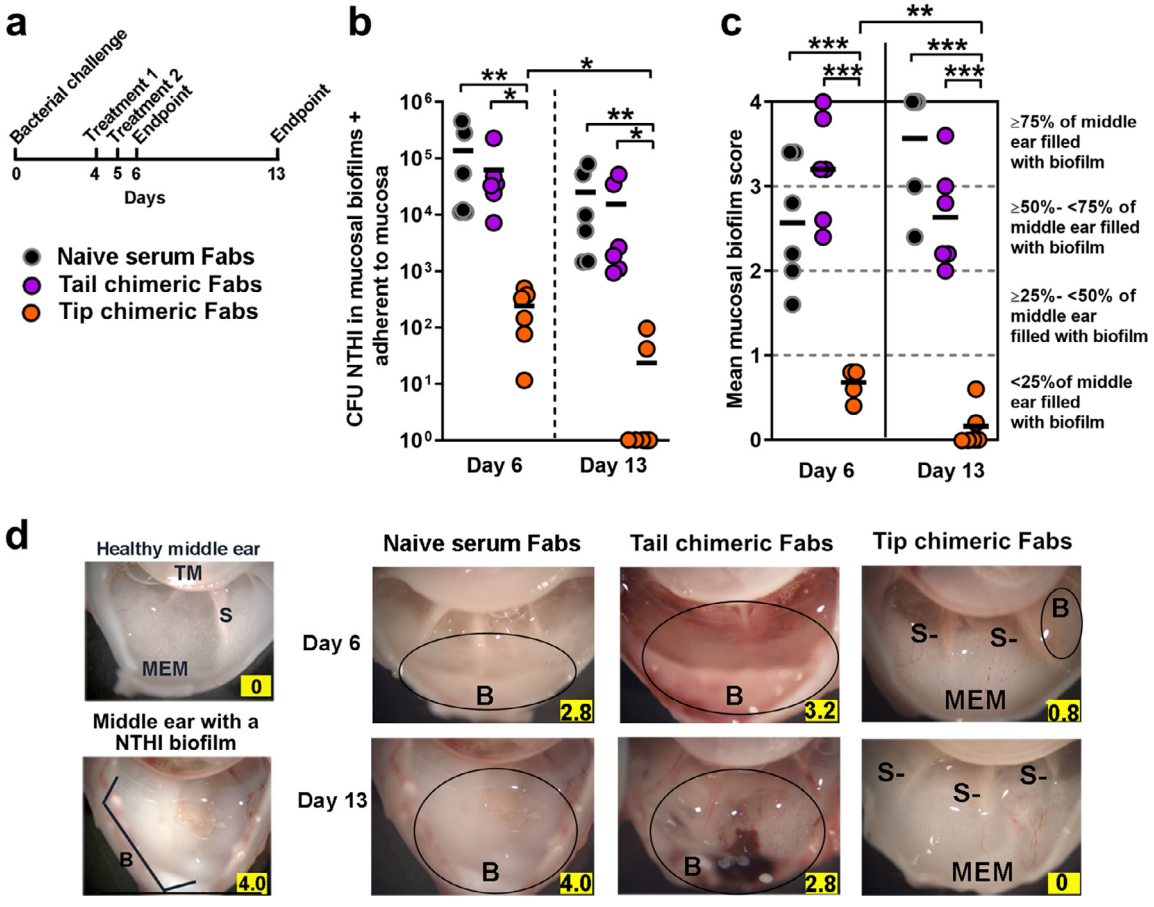

Fig. 4. Tip chimeric Fabs from polyclonal rabbit IgG mediated clearance of biofilm resident NTHI, eradication of established mucosal biofilms and resolution of experimental disease. (a) Study timeline. A dose of 342 nM Fabs was delivered into each middle ear. (b) Relative quantity of NTHI resident within mucosal biofilms and adherent to the middle ear mucosa one or seven days after completion of antibody therapy. (c) Relative amount of remaining mucosal biofilm as determined by six reviewers blinded to treatment delivered. Panels b and c: 6 middle ears per cohort, values for individual ears and mean for each cohort shown. $^{*}P \leq 0.05$, $^{**}P \leq 0.01$, $^{***}P \leq 0.001$ [one-way ANOVA with multiple comparisons]. (d) Representative images of middle ear mucosal biofilms; mean mucosal biofilm score indicated within yellow box. TM, tympanic membrane; S, bony septae; MEM, middle ear mucosa; B, biofilm (encircled).

remained within the middle ears after treatment on a 0–4+ scale. Receipt of tail chimeric peptide Fabs was not effective. One day after treatment in animals that received tail chimeric peptide Fabs, the remaining biofilms were actually slightly larger than those in the middle ears of animals treated with naive serum Fabs, with mean biomass scores of 3.2 and 2.6, respectively [Fig. 4c]. In both of these negative control cohorts, >50% of the middle ear remained filled with mucosal biofilm. Conversely, in the cohort given tip chimeric peptide Fabs, all six middle ears were ranked ≤1.0 which indicated only minimal remaining mucosal biofilm was observed ($P \leq 0.001$; one-way ANOVA with multiple comparisons), with a mean biomass score of 0.7. Thus, the immediate outcome of tip chimeric peptide Fab therapy was significant reduction of bacterial load and significant disruption of established NTHI biofilms.

To assay the durability of the observed treatment effect, middle ears were evaluated in a subset of each cohort after an additional week, without any further treatment. In the cohort given Fabs from naive rabbit serum, mucosal biofilms actually increased, whereas they only slightly decreased in those given tail chimeric peptide Fabs (*e.g.* >50% of the middle ears remained filled with an NTHI biofilm), with mean biomass scores of 3.6 and 2.6, respectively [Fig. 4c]. Importantly, animals treated with tip chimeric peptide Fabs continued to clear NTHI biofilms, as evidenced by an additional significant reduction in mucosal biofilm ($P \leq 0.01$; one-way ANOVA with multiple comparisons) and a mean biomass score of 0.2. Notably, there was no visible evidence of a biofilm in 4 of 6 (67%) middle ears. These qualitative assessments correlated well with bacterial load data as shown in Fig. 4b.

To demonstrate what blinded evaluators ranked in terms of remaining mucosal biofilms observed, examples of a healthy middle ear and one with a four-day NTHI biofilm as well as representative images of middle ears from each cohort on day 13 are depicted in Fig. 4d. As anticipated, one day after completion of treatment, substantial mucosal biofilm remained in animals that received naive serum or tail chimeric peptide Fabs, as evidenced by the fact that these biofilms occluded visibility of the middle ear mucosa and bony septae, with representative assigned scores of 2.8 or 3.2 respectively [Fig. 4d]. These scores did not decrease significantly by seven days after treatment completion and in fact, that for the cohort treated with naive serum Fabs increased notably, with representative assigned scores of 4.0 and 2.8, respectively. Conversely, in the middle ears of animals treated with tip chimeric peptide Fabs, the normal anatomical landmarks were fully visible one day after treatment completion and remained so, with no evidence of biofilm regrowth in the seven days that followed. Representative assigned scores were 0.8 (day 6) and 0 (day 13) for this latter cohort. Collectively, these data provided additional strong support for the potential to deliver tip chimeric peptide Fabs to eradicate existing NTHI biofilms within the middle ear, and further that this eradication was likely enduring.

3.4. Development and validation of a humanised version of the tip chimeric peptide monoclonal antibody

With data in support of use of anti-tip chimeric peptide Fabs to disrupt diverse bacterial biofilms *in vitro*, and to also eradicate mucosal NTHI biofilms *in vivo*, we now wanted to move toward use of these novel therapeutic agents in clinical trials. To do so, we generated a panel of humanised tip chimeric peptide-directed monoclonal antibodies (herein called 'HuTipMab') designed after a murine monoclonal antibody against the tip chimeric peptide. Here, we present data in support of the functional *in vitro* activity of one of the HuTipMabs as evidence of the effectiveness of humanisation. As a measure of humanness, we determined the T20 score for the variable regions within the heavy and light chains individually [37]. These values were 82 for the heavy chain variable region and 97 for the light chain variable region, which indicated a high degree of humanness for each antibody domain. By surface plasmon resonance, the HuTipMab had a K_D of 76 nM to the tip chimeric peptide and a K_D of 10 nM to native $IHF_{N\text{-}THI}$, thus strong affinity to the target peptide, and even greater affinity to the native protein (as would be needed for disease resolution) was shown. *In vitro*, HuTipMab significantly disrupted biofilms formed by NTHI, *P. aeruginosa* or *B. cenocepacia* ($P \leq 0.001$; unpaired *t*-test) [Fig. 5a] and only 13–26% biofilm biomass remained after a 16 h exposure to the selected concentration of humanised Mab used, compared to biofilms incubated with an equivalent concentration of humanised anti-tail chimeric peptide antibody (called 'HuTailMab') [Fig. 5b]. Thus, humanisation of a murine tip chimeric peptide-specific monoclonal

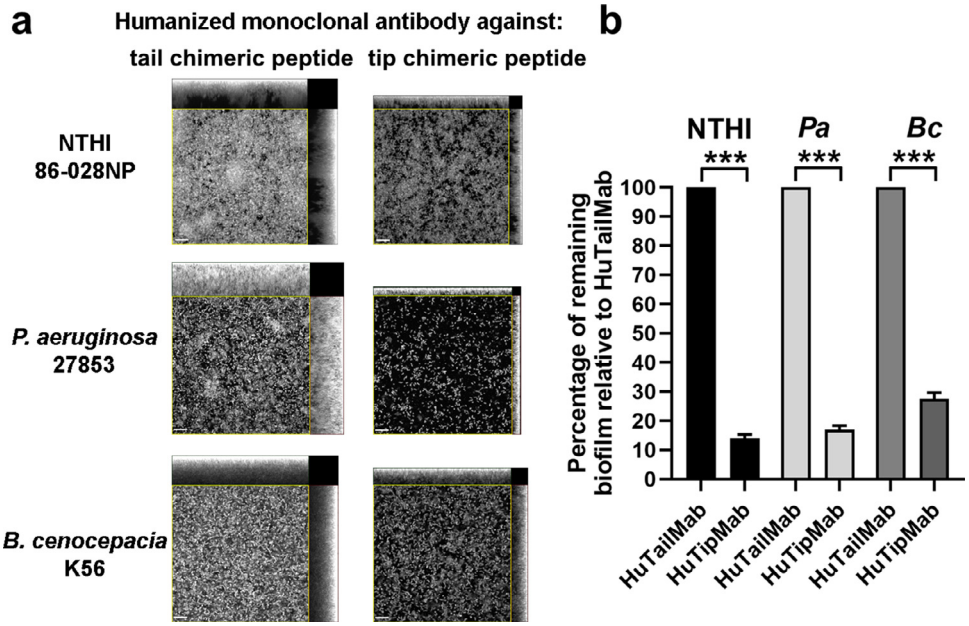

Fig. 5. A humanised tip chimeric peptide monoclonal antibody disrupted bacterial biofilms *in vitro*. (a) Representative images of bacterial biofilms (pseudocoloured white) after 16 h incubation with HuTipMab or HuTailMab. Orthogonal projections show a top-down view to depict spatial distribution of biofilm in x-y plane and side view indicates biofilm height in z-plane. Scale bars, 20 μm. (b) Percentage of biofilm biomass that remained after exposure to HuTipMab compared to HuTailMab, determined by COMSTAT2 analysis. Mean ± SD shown. Experiments were performed three times on separate days. $^{***}P \leq 0.001$ [unpaired *t*-test].

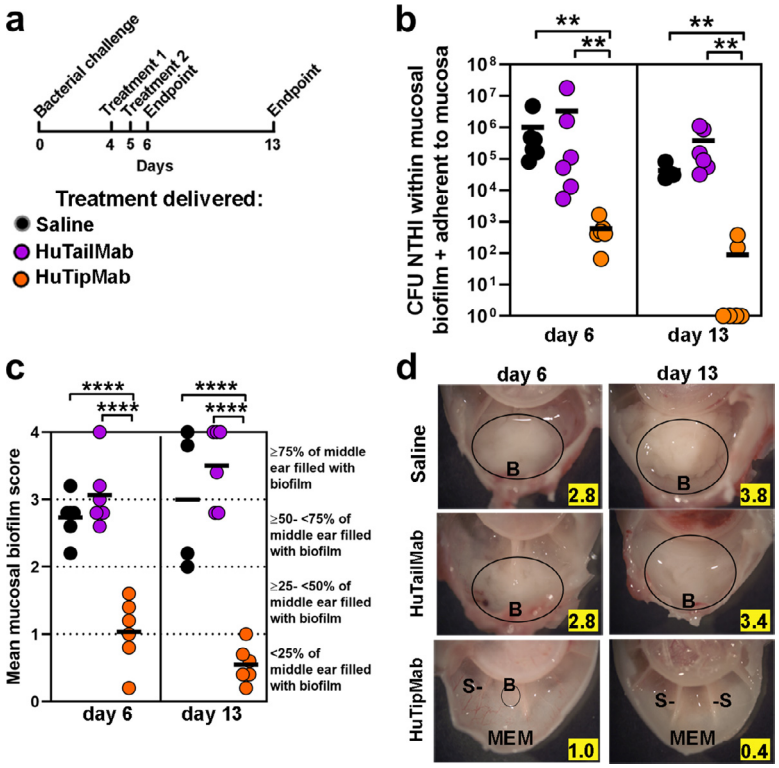

Fig. 6. A humanised monoclonal antibody against the tip chimeric peptide resolved pre-existing NTHI biofilms present in the middle ears during experimental NTHI-induced OM. (a) Study timeline and treatments. (b) Relative quantity of NTHI within the middle ear. (c) Relative amount of NTHI mucosal biofilm that remained in the middle ear after treatment with humanised monoclonal antibodies. Panels b and c: six middle ears per cohort, values for individual ears and mean for cohort shown. $^{****}P \leq 0.0001$ [One-way ANOVA with multiple comparisons]. (d) Representative images of middle ears from each cohort; mean mucosal biofilm score for the ear indicated within yellow box. S, bony septae; MEM, middle ear mucosa; B, biofilm, encircled.

antibody yielded a therapeutic candidate with strong affinity to its protein target and proven ability to disrupt biofilms formed by three human respiratory tract pathogens *in vitro*.

To next confirm that the humanised monoclonal also functioned *in vivo*, we again used the chinchilla model of NTHI-induced experimental OM wherein biofilms were already resident within the middle ears prior to treatment. We delivered either HuTipMab, HuTailMab or an equivalent volume of sterile saline (diluent used with humanised antibodies) to both middle ears, followed 24 h later by a second identical treatment [Fig. 6a]. As before, a subset of animals from each cohort was sacrificed one day after therapy was completed to examine the immediate outcome, and a second subset of animals were followed for another week without additional treatment to determine if the effect of therapy endured.

One day after therapy, HuTipMab induced a significant >3.5 log reduction in the number of NTHI, compared to HuTailMab or saline ($P \leq 0.01$; one-way ANOVA with multiple comparisons) [Fig. 6b]. One week later, whereas either HuTailMab or saline induced only a slight additional decrease in NTHI load, that in middle ears treated with HuTipMab decreased another 7-fold. Notably, a week after treatment with HuTipMab, homogenates of 4 of 6 middle ear mucosae (67%) were culture-negative ($P \leq 0.05$; one-way ANOVA with multiple comparisons). Thus, treatment with HuTipMab induced rapid eradication of NTHI within mucosal biofilms from the middle ear.

To qualitatively assess how much mucosal biofilm remained in the middle ear after treatment, middle ears were once again blindly evaluated on a 0–4+ scale. Animals that received saline or HuTailMab remained filled with mucosal biofilm that occupied >50% of the middle ear, and mean biomass scores were 2.7 and 3.1, respectively [Fig. 6c]. Conversely, in those middle ears treated with HuTipMab, minimal remaining mucosal biofilm was observed (<25%) and the mean biomass score for the cohort was 1.0 [Fig. 6c]. Seven days later, whereas the mucosal biofilm actually increased in cohorts treated with either saline (mean score, 3.0) or HuTailMab (mean score, 3.5), in those treated with the HuTipMab minimal biofilm (mean score, 0.6) was observed. Representative images for each cohort are shown in Fig. 6d and correlated well with data presented in Fig. 6c.

Unlike in Figs. 2d and 4d, wherein notable inflammation had been visible in the middle ears of animals that received either Fabs derived from a murine monoclonal antibody directed exclusively at the β-tail of one of the IHF sub-units, or those that received Fabs derived from a rabbit polyclonal directed at the tail chimeric peptide, we did not observe a similar degree of inflammatory changes once we humanised the monoclonal directed against the tail chimeric peptide. Whereas some inflammation was noted in animals treated with the HuTailMab, this sign was abrogated (see Fig. 6d, images in middle row). To begin to explain this observation, we again performed a cytometric bead assay to determine a focused but now slightly expanded cytokine profile within middle ear fluids collected from these animals at the time of sacrifice. One day after completion of antibody therapy, whereas there was a significantly reduced quantity of each of six proinflammatory cytokines detected in middle ear fluids from animals that received HuTipMab, there was now a comparable quantity of pro-inflammatory cytokines in the middle ear fluids recovered from animals that had received either saline or HuTailMab [Fig. 7a]. Moreover, significantly more of two anti-inflammatory cytokines were detected in middle ear fluids recovered from animals that received HuTipMab, whereas these values were again comparable in the cohorts that had been treated with either saline or HuTailMab. These patterns were maintained and further enhanced within fluids collected on day 13 (7 days after completion of therapy) [Fig. 7b]. As pro-inflammatory cytokine concentrations were now comparable between saline and HuTailMab-treated animals, we theorise that humanisation of the tail-directed monoclonal antibody abrogated the

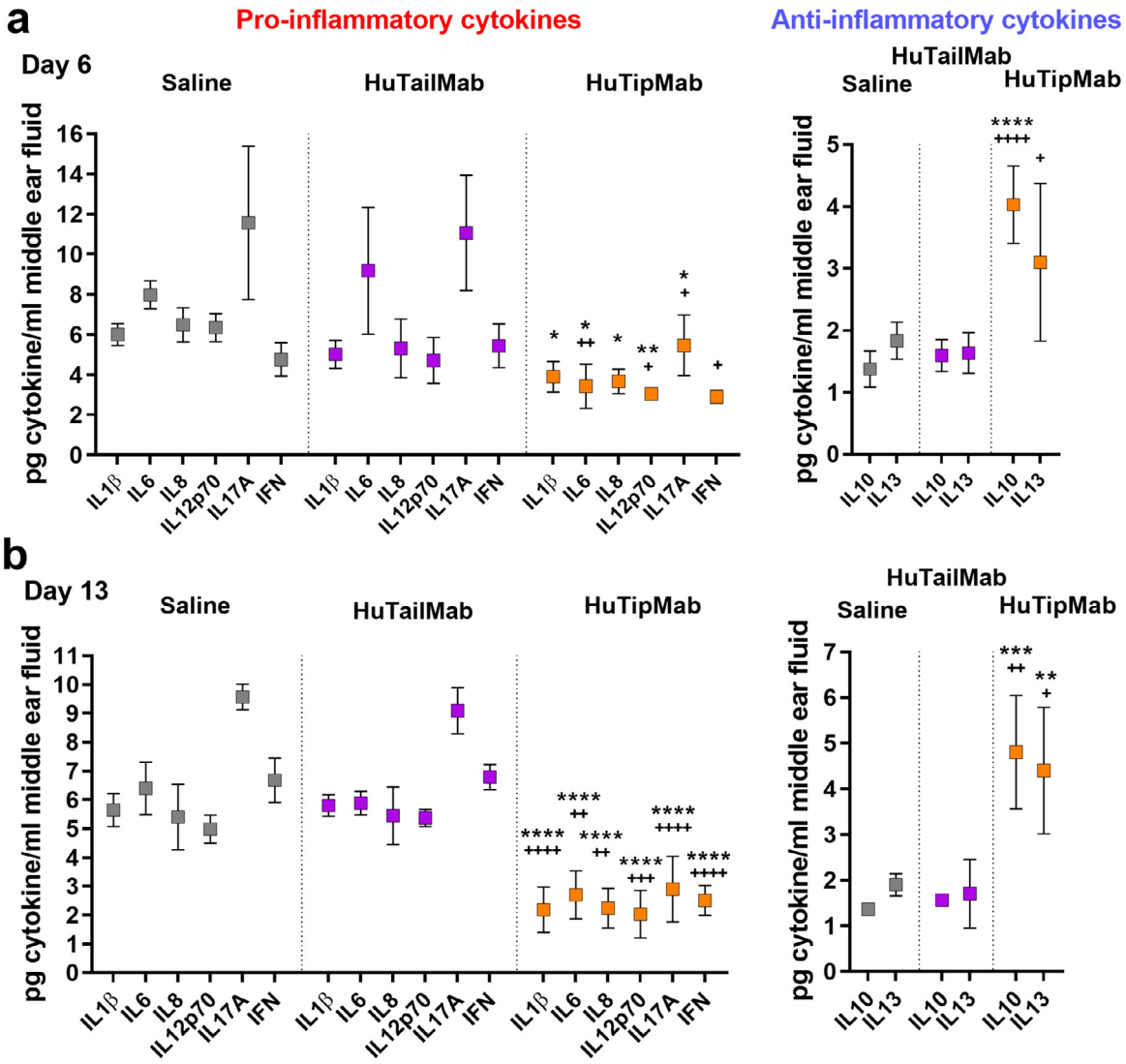

Fig. 7. Pro-inflammatory cytokines were significantly less abundant in middle ear fluids from animals treated with HuTipMabs. Relative quantity of pro-inflammatory and anti-inflammatory cytokines in chinchilla middle ear fluids after NTHI challenge and treatment with humanised monoclonal antibodies (a) six days after NTHI challenge (one day after completion of therapy) and (b) 13 days after NTHI challenge (seven days after completion of therapy) as determined by cytometric bead array. $^{*}P \leq 0.05$ *vs.* saline, $^{**}P \leq 0.01$ *vs.* saline, $^{***}P \leq 0.001$ *vs.* saline, $^{****}P \leq 0.0001$ *vs.* saline, $^{+}P \leq 0.05$ *vs.* HuTailMab,$^{++}P \leq 0.01$ *vs.* HuTailMab, $^{++}P \leq 0.001$ *vs.* HuTailMab, $^{++++}P \leq 0.0001$ *vs.* HuTailMab [one-way ANOVA with multiple comparisons]. 3 to 5 middle ear fluids tested per cohort. Mean cytokine concentration ± SD shown.

inflammation induced by treatment of animals with Fabs generated from either murine anti-β tail or rabbit anti-tail chimeric peptide sera (compare Fig. 6d to Figs. 2d or 4d). Collectively, these data demonstrated that humanisation of the murine monoclonal directed against the tip chimeric peptide did not diminish its effectiveness either *in vitro* or *in vivo*. The HuTipMab induced rapid and enduring clearance of NTHI-induced mucosal biofilms from the middle ear during experimental OM, thus fostering resolution of disease.

3.5. *Pre-clinical efficacy of the tip chimeric peptide after active transcutaneous immunisation*

Thus far, we have reported development of an effective DNABII-targeted therapeutic (*e.g.* delivery of a humanised monoclonal antibody that targets the immunoprotective tip regions of both IHF subunits to disrupt biofilms/resolve ongoing disease), however prevention of biofilm formation and disease induction by active immunisation is also an important goal. Toward this end, we now used a unique chinchilla viral-bacterial co-infection model of experimental OM wherein prior adenovirus infection predisposes the middle ear to invasion by NTHI that colonise the nasopharynx which now ascend the virus-compromised Eustachian tube [32]. This superinfection model is designed to mimic "*My child gets a cold, then a week later has an ear infection*". Thus, animals were first actively immunised with the tip or tail chimeric peptide to induce the appropriate immune response [31,33,35,38]. Subsequently, chinchillas were challenged first with adenovirus, then 7-days later with NTHI, after which they were monitored for relative development of ascending OM.

Three cohorts of naive chinchillas were immunised by rubbing vaccine formulations on to the skin just behind both ears (*e.g.* post-auricular region), a procedure repeated one week later [Fig. 8a]. Formulations used were: tip chimeric peptide admixed with the adjuvant dmLT, a double mutant of *E. coli* heat labile enterotoxin [34]; tail chimeric peptide plus dmLT; or dmLT alone. Two days after the second immunisation, all animals were inoculated intranasally (IN) with adenovirus, followed one week later by IN challenge with NTHI. Nasopharyngeal lavage was performed one day after NTHI challenge to confirm that all animals were equivalently colonised [Fig. 8b]. This result ensured that each animal had the potential to develop

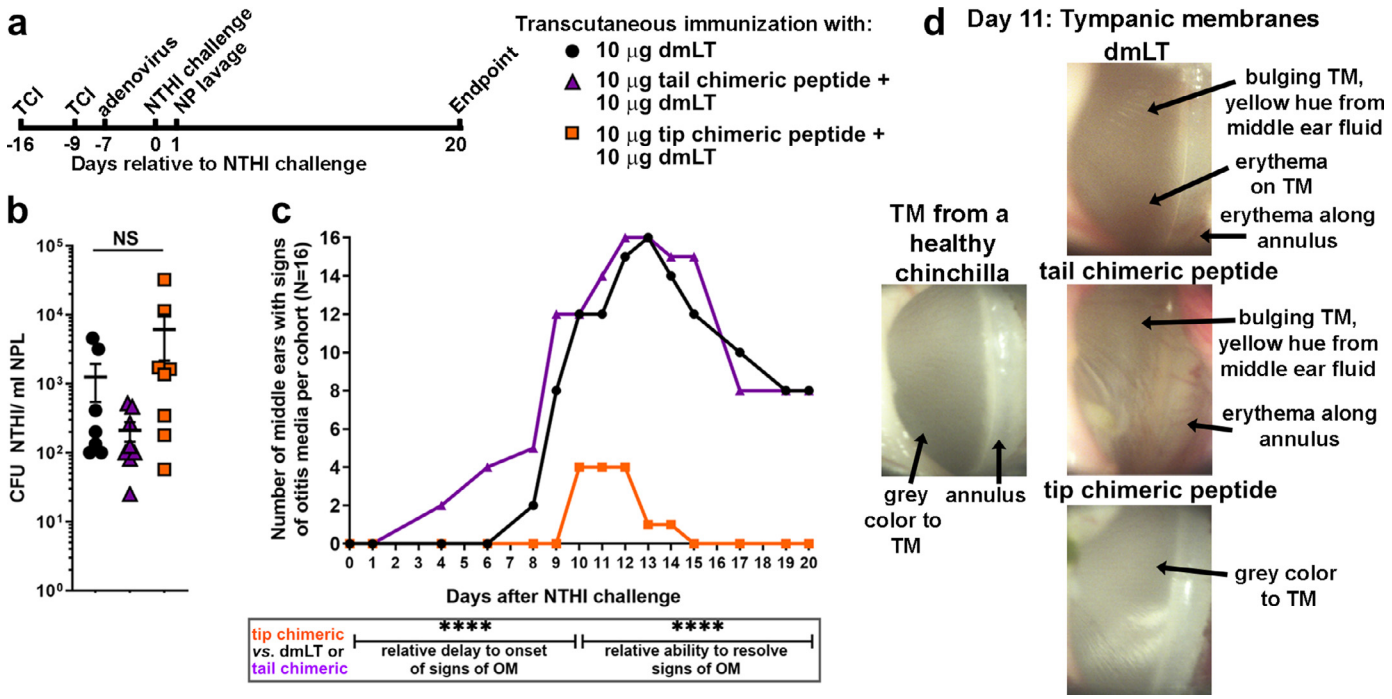

Fig. 8. Immunisation with tip chimeric peptide prevented ascending experimental OM in a viral-bacterial co-infection model. (a) Study timeline and vaccine formulations delivered. (b) Relative quantity of NTHI within nasopharyngeal lavage fluids one day after bacterial challenge to ensure all cohorts were equivalently colonised. 8 lavage fluids per cohort, NS, no significance [one-way ANOVA]. (c) Number of animals in each cohort with signs of experimental OM, *i.e.* inflammation and/or middle ear fluid, visualised by blinded video otoscopy. Eight animals per cohort, $^{****}P \leq 0.001$ vs. dmLT or tail chimeric peptide [Mantel–Cox test]. (d) Representative images of tympanic membranes from each cohort on day 11, which was the day of maximum disease incidence in the cohort immunised with the tip chimeric peptide. TM, tympanic membrane.

experimental OM, with the only discriminating factor being resultant induced immunity due to immunogen received.

The primary readout for vaccine efficacy was video otoscopy, wherein each tympanic membrane (TM) was blindly viewed to determine whether overt inflammation and middle ear fluid were visible as signs of OM [36]. Within 8 days of NTHI challenge of virus-infected chinchillas, there were signs of that NTHI had ascended the compromised Eustachian tube and induced OM in 2 of 16 middle ears (13%) in the adjuvant-only cohort, with a peak incidence of 100% on day 13 [Fig. 8c]. Experimental OM began to decrease after day 13 but persisted in 8 of 16 middle ears (50%) on day 20. As anticipated, immunisation with tail chimeric peptide did not provide a benefit. Signs of OM were present in two middle ears (13%) four days after NTHI challenge, peaked at 100% on days 12 and 13 before beginning to decline, however 8 of 16 middle ears (50%) maintained signs of OM at study conclusion. In sharp contrast, there was a significant delay to onset of signs of OM in the tip chimeric peptide-immunised cohort ($P \leq 0.0001$; Mantel-Cox test) until day 10. Maximum incidence of OM on days 10 to 12 occurred in only 4 of 18 middle ears (25%) in this latter cohort with complete resolution by day 14, which was significantly earlier than controls ($P \leq 0.0001$; Mantel-Cox test). Further, over the 20-day observation period, the proportion of animals with signs of experimental OM was significantly less in those immunised with the tip chimeric peptide (4 ears; 2 animals; $P \leq 0.0001$; Mantel-Cox test) compared to the other two cohorts (16 ears; 8 animals).

Images of the chinchilla TM shown in Fig. 8d are representative of that observed by blinded otoscopy on day 11. Whereas a healthy chinchilla TM is grey in colour, those of animals immunised with dmLT or the tail chimeric peptide were slightly bulging, erythematous and yellow middle ear fluid was visible behind the TM. Conversely, TMs of the majority of animals in the tip chimeric peptide immunised cohort (12 of 16; 75%) showed minimal, if any, signs of inflammation. Overall, vaccine efficacy afforded by immunisation with the tip chimeric peptide was 85%, compared to either negative control cohort. Collectively, these data supported the design and use of the tip chimeric peptide as an effective vaccine candidate antigen to prevent development of experimental OM due to NTHI and complemented our development of a therapeutic humanised monoclonal antibody.

4. Discussion

Biofilms are involved in the majority of chronic and recurrent bacterial diseases of the respiratory tract [39–41], oral cavity [42,43], gastrointestinal tract[44,45] and urogenital tract [46,47]. The formation and persistence of these often polymicrobial communities contributes significantly to the pathogenesis of these diseases, largely due to a characteristic recalcitrance to clearance by host immune effectors and antibiotics. Thus, recognition of the role of biofilms in disease pathogenesis and persistence requires novel approaches to either prevent their formation or eradicate those already present.

As such, many laboratories have developed a variety of approaches for biofilm mitigation which has been the subject of many excellent reviews[10,48–51]. A broad area of research is focused on biofilm eradication via agents that induce dispersal of biofilm-resident bacteria, *e.g.* treatment of biofilms with enzymes, molecules that interfere with processes such as quorum sensing, signaling via cyclic di-GMP or delivery of small molecule inhibitors or analogues [10,48–51]. Alternatively, prevention of biofilm formation is an approach that could also restrict disease-induced inflammation, which is often more damaging to the host compared to the presence of the biofilm itself [52]. Modification of implantable devices or incorporation of inhibitors within biomaterials, use of antimicrobial peptides or blockade of adhesive proteins expressed by microorganisms are shown to limit biofilm formation [53–56].

With regard to our own approach, over the past 10+ years, since we identified the structural eDNA+DNABII lattice within biofilms formed by NTHI in the chinchilla middle ear [11], we and others have expanded this observation to demonstrate the presence of this bacterial-permissive, but host-restrictive lattice in biofilms formed by many diverse bacterial species, including the high priority ESKAPE

pathogens [16–23]. Collectively, this observation initially made *in vitro*, then expanded to testing in multiple pre-clinical models [11–13,18,21] supported our development of a novel DNABII-focused approach to mediate biofilm diseases that would target this seemingly species-independent 'Achilles heel'.

As such, we devised a two-pronged approach. First, we designed an epitope-specific DNABII chimeric peptide vaccine candidate antigen to induce the formation of antibodies that would prevent biofilm formation after active immunisation. Second, we humanised a murine monoclonal antibody against this immunogen for use, either intact or as Fab fragments, as a broadly effective therapeutic wherein bacteria released from biofilm residence could then be killed by host immune effectors and/or antibiotics, although now able to be used at a greatly reduced dose [6–8]. Here we presented promising preclinical evidence from four studies, using two distinct models of OM, which consistently showed how effective these approaches can be in terms of biofilm and disease prevention and/or marked and significant reduction of existing mucosal biofilms with rapid disease resolution.

Herein, we provide answers to several previously unanswered questions. We found that Fab fragments were as effective as intact antibody to disrupt biofilms *in vitro* and *in vivo* and could thus serve as a therapeutic when repeated dosing might be required (due to a related concern about inducing an anti-antibody response). We also determined that the Fc portion of a DNABII-directed antibody was not required for biofilm disruption *in vitro* or for biofilm resolution *in vivo*. This outcome suggested that release of bacteria from the protective biofilm would be sufficient to promote clearance and disease resolution by innate host immune effectors and/or antibiotics. We learned that incorporating protective domains from both of the heterogeneous subunits of IHF_{NTHI} did result in the anticipated increased efficacy. Further, active immunisation with the tip chimeric peptide induced the formation of antibody that prevented development of experimental OM and promoted rapid disease resolution. Humanisation of the tip chimeric peptide monoclonal antibody yielded a highly promising lead therapeutic with nanomolar affinity to both the immunogen and native protein, the latter of which is required for clinical efficacy.

Collectively, these new data added to our understanding of the eDNA+DNABII-directed strategy and were highly supportive of entry into both preventative and therapeutic clinical trials of the tip chimeric peptide immunogen and the humanised monoclonal antibody against it, respectively. Given the species-independent nature of our DNABII targeted approach, we hope to contribute a broadly effective candidate vaccine antigen and therapeutic product for improved clinical management of a multitude of diseases wherein pathogenesis, enduring chronicity and/or cyclical recurrence is due to a recalcitrant biofilm.

Acknowledgements

We thank Joseph A. Jurcisek, Stephen L. Toone and Dr. Kenneth L. Brockman for technical assistance and Jennifer Neelans for manuscript preparation.

Funding source

This work was supported by R01 DC011818 to LOB and SDG. The funding source had no role in study design; in the collection, analysis, and interpretation of data; in the writing of the report; and in the decision to submit the paper for publication.

Declaration of Competing Interest

Dr. Bakaletz reports grants from National Institutes of Health, during the conduct of the study; In addition, Dr. Bakaletz has a pending patent U.S. Provisional App. 62/455,437 licensed to Clarametyx Biosciences, Inc., a pending patent PCT/US2018/012235 licensed to Clarametyx Biosciences, Inc., a pending patent U.S. App. 16/475,656 licensed to Clarametyx Biosciences, Inc., a pending patent Australia App. 2018206552 licensed to Clarametyx Biosciences, Inc., a pending patent Canada App. CA3049105 licensed to Clarametyx Biosciences, Inc., a pending patent Europe App. 18701943.5 licensed to Clarametyx Biosciences, Inc., a pending patent Japan App. 2019−556567 licensed to Clarametyx Biosciences, Inc., and a pending patent U.S. Provisional App. 62/871,457 licensed to Clarametyx Biosciences, Inc. and L.O.B. is an inventor of technology related to the DNABII-directed approach, rights to which have been licensed to Clarametyx Biosciences, Inc.

Dr. Goodman reports grants from National Institutes of Health, during the conduct of the study; In addition, Dr. Goodman has a pending patent U.S. Provisional App. 62/455,437 licensed to Clarametyx Biosciences, Inc., a pending patent PCT/US2018/012235 licensed to Clarametyx Biosciences, Inc., a pending patent U.S. App. 16/475,656 licensed to Clarametyx Biosciences, Inc., a pending patent Australia App. 2018206552 licensed to Clarametyx Biosciences, Inc., a pending patent Canada App. CA3049105 licensed to Clarametyx Biosciences, Inc., a pending patent Europe App. 18701943.5 licensed to Clarametyx Biosciences, Inc., a pending patent Japan App. 2019-556567 licensed to Clarametyx Biosciences, Inc., and a pending patent U.S. Provisional App. 62/871,457 licensed to Clarametyx Biosciences, Inc. and S.D.G. is an inventor of technology related to the DNABII-directed approach, rights to which have been licensed to Clarametyx Biosciences, Inc.

Dr. Novotny has nothing to disclose.

Author contributions

LOB & LAN designed the studies, LAN conducted the experiments, LOB & SDG provided materials; LAN & LOB analysed the experimental data; LAN & LOB drafted the manuscript; LAN, LOB & SDG approved the final manuscript version.

Supplementary materials

Supplementary material associated with this article can be found, in the online version, at doi:10.1016/j.ebiom.2020.102867.

References

[1] Bates A, Power CA. David *vs.* Goliath: the structure, function, and clinical prospects of antibody fragments. Antibodies 2019;8:28.
[2] Dongari-Bagtzoglou A. Mucosal biofilms: challenges and future directions. Expert Rev Anti Infect Ther 2008;6:141–4.
[3] Costerton JW. Overview of microbial biofilms. J Ind Microbiol 1995;15:137–40.
[4] Donlan RM. Biofilms: microbial life on surfaces. Emerg Infect Dis 2002;8:881–90.
[5] Flemming HC, Neu TR, Wozniak DJ. The EPS matrix: the "house of biofilm cells". J Bacteriol 2007;189:7945–7.
[6] Shigeta M, Komatsuzawa H, Sugai M, Suginaka H, Usui T. Effect of the growth rate of *Pseudomonas aeruginosa* biofilms on the susceptibility to antimicrobial agents. Chemotherapy 1997;43:137–41.
[7] Lewis DM. A simple model of plankton population dynamics coupled with a LES of the surface mixed layer. J Theor Biol 2005;234:565–91.
[8] Singh S, Singh SK, Chowdhury I, Singh R. Understanding the mechanism of bacterial biofilms resistance to antimicrobial agents. Open Microbiol J 2017;11:53–62.
[9] Rabin N, Zheng Y, Opoku-Temeng C, Du Y, Bonsu E, Sintim HO. Biofilm formation mechanisms and targets for developing antibiofilm agents. Future Med Chem 2015;7:493–512.
[10] Verderosa AD, Totsika M, Fairfull-Smith KE. Bacterial biofilm eradication agents: a current review. Front Chem 2019;7:824.
[11] Goodman SD, Obergfell KP, Jurcisek JA, et al. Biofilms can be dispersed by focusing the immune system on a common family of bacterial nucleoid-associated proteins. Mucosal Immunol 2011;4:625–37.
[12] Brockson ME, Novotny LA, Mokrzan EM, et al. Evaluation of the kinetics and mechanism of action of anti-integration host factor-mediated disruption of bacterial biofilms. Mol Microbiol 2014;93:1246–58.
[13] Novotny LA, Goodman SD, Bakaletz LO. Redirecting the immune response towards immunoprotective domains of a DNABII protein resolves experimental otitis media. NPJ Vaccines 2019;4:43.
[14] Jurcisek JA, Bakaletz LO. Biofilms formed by nontypeable *Haemophilus influenzae in vivo* contain both double-stranded DNA and type IV pilin protein. J Bacteriol 2007;189:3868–75.

[15] Mokrzan EM, Novotny LA, Brockman KL, Bakaletz LO. Antibodies against the majority subunit (PilA) of the type IV pilus of nontypeable *Haemophilus influenzae* disperse *Moraxella catarrhalis* from a dual-species biofilm. MBio 2018;9 e02423-18.
[16] Abu Khweek A, Fernandez Davila NS, Caution K, et al. Biofilm-derived *Legionella pneumophila* evades the innate immune response in macrophages. Front Cell Infect Microbiol 2013;3:18.
[17] Devaraj A, Justice SS, Bakaletz LO, Goodman SD. DNABII proteins play a central role in UPEC biofilm structure. Mol Microbiol 2015;96:1119–35.
[18] Freire MO, Devaraj A, Young A, et al. A bacterial-biofilm-induced oral osteolytic infection can be successfully treated by immuno-targeting an extracellular nucleoid-associated protein. Mol Oral Microbiol 2017;32:74–88.
[19] Gustave JE, Jurcisek JA, McCoy KS, Goodman SD, Bakaletz LO. Targeting bacterial integration host factor to disrupt biofilms associated with cystic fibrosis. J Cyst Fibros 2013;12:384–9.
[20] Novotny LA, Amer AO, Brockson ME, Goodman SD, Bakaletz LO. Structural stability of *Burkholderia cenocepacia* biofilms is reliant on eDNA structure and presence of a bacterial nucleic acid binding protein. PLoS One 2013;8:e67629.
[21] Novotny LA, Jurcisek JA, Goodman SD, Bakaletz LO. Monoclonal antibodies against DNA-binding tips of DNABII proteins disrupt biofilms *in vitro* and induce bacterial clearance *in vivo*. EBioMedicine 2016;10:33–44.
[22] Rocco CJ, Bakaletz LO, Goodman SD. Targeting the HUβ protein prevents *Porphyromonas gingivalis* from entering into preexisting biofilms. J Bacteriol 2018;200: e00790-17.
[23] Rood KM, Buhimschi IA, Jurcisek JA, et al. Skin microbiota in obese women at risk for surgical site infection after Cesarean delivery. Sci Rep 2018;8:8756.
[24] Idicula WK, Jurcisek JA, Cass ND, et al. Identification of biofilms in post-tympanostomy tube otorrhea. Laryngoscope 2016;126:1946–51.
[25] Swinger KK, Rice PA. IHF and HU: flexible architects of bent DNA. Curr Opin Struct Biol 2004;14:28–35.
[26] Bakaletz LO, Tallan BM, Hoepf T, DeMaria TF, Birck HG, Lim DJ. Frequency of fimbriation of nontypable *Haemophilus influenzae* and its ability to adhere to chinchilla and human respiratory epithelium. Infect Immun 1988;56:331–5.
[27] Luke NR, Russo TA, Luther N, Campagnari AA. Use of an isogenic mutant constructed in *Moraxella catarrhalis* to identify a protective epitope of outer membrane protein B1 defined by monoclonal antibody 11C6. Infect Immun 1999;67:681–7.
[28] Mahenthiralingam E, Coenye T, Chung JW, et al. Diagnostically and experimentally useful panel of strains from the *Burkholderia cepacia* complex. J Clin Microbiol 2000;38:910–3.
[29] Jurcisek JA, Dickson AC, Bruggeman ME, Bakaletz LO. *In vitro* biofilm formation in an 8-well chamber slide. J Vis Exp 2011:2481.
[30] Heydorn A, Nielsen AT, Hentzer M, et al. Quantification of biofilm structures by the novel computer program COMSTAT. Microbiology 2000;146(Pt 10):2395–407.
[31] Novotny LA, Clements JD, Bakaletz LO. Transcutaneous immunization as preventative and therapeutic regimens to protect against experimental otitis media due to nontypeable *Haemophilus influenzae*. Mucosal Immunol 2011;4:456–67.
[32] Suzuki K, Bakaletz LO. Synergistic effect of adenovirus type 1 and nontypeable *Haemophilus influenzae* in a chinchilla model of experimental otitis media. Infect Immun 1994;62:1710–8.
[33] Novotny LA, Clements JD, Goodman SD, Bakaletz LO. Transcutaneous immunization with a band-aid prevents experimental otitis media in a polymicrobial model. Clin Vaccine Immunol 2017;24 e00563-16.
[34] Clements JD, Norton EB. The mucosal vaccine adjuvant LT(R192G/L211A) or dmLT. mSphere 2018;3:e00215–8.
[35] Novotny LA, Clements JD, Bakaletz LO. Kinetic analysis and evaluation of the mechanisms involved in the resolution of experimental nontypeable *Haemophilus influenzae*-induced otitis media after transcutaneous immunization. Vaccine 2013;31:3417–26.
[36] Novotny LA, Jurcisek JA, Godfroid F, Poolman JT, Denoel PA, Bakaletz LO. Passive immunization with human anti-protein D antibodies induced by polysaccharide protein D conjugates protects chinchillas against otitis media after intranasal challenge with *Haemophilus influenzae*. Vaccine 2006;24:4804–11.
[37] Gao SH, Huang K, Tu H, Adler AS. Monoclonal antibody humanness score and its applications. BMC Biotechnol 2013;13:55.
[38] Novotny LA, Clements JD, Bakaletz LO. Therapeutic transcutaneous immunization with a band-aid vaccine resolves experimental otitis media. Clin Vaccine Immunol 2015;22:867–74.
[39] Bakaletz LO. Bacterial biofilms in the upper airway - evidence for role in pathology and implications for treatment of otitis media. Paediatr Respir Rev 2012;13:154–9.
[40] Fastenberg JH, Hsueh WD, Mustafa A, Akbar NA, Abuzeid WM. Biofilms in chronic rhinosinusitis: pathophysiology and therapeutic strategies. World J Otorhinolaryngol Head Neck Surg 2016;2:219–29.
[41] Costerton JW. Cystic fibrosis pathogenesis and the role of biofilms in persistent infection. Trends Microbiol 2001;9:50–2.
[42] Bowen WH, Burne RA, Wu H, Koo H. Oral biofilms: pathogens, matrix, and polymicrobial interactions in microenvironments. Trends Microbiol 2018;26:229–42.
[43] Petersen PE, Ogawa H. Strengthening the prevention of periodontal disease: the WHO approach. J Periodontol 2005;76:2187–93.
[44] von Rosenvinge EC, O'May GA, Macfarlane S, Macfarlane GT, Shirtliff ME. Microbial biofilms and gastrointestinal diseases. Pathog Dis 2013;67:25–38.
[45] Macfarlane S, Dillon JF. Microbial biofilms in the human gastrointestinal tract. J Appl Microbiol 2007;102:1187–96.
[46] Flores-Mireles AL, Walker JN, Bauman TM, et al. Fibrinogen release and deposition on urinary catheters placed during urological procedures. J Urol 2016;
196:416–21.
[47] Tenke P, Koves B, Nagy K, et al. Update on biofilm infections in the urinary tract. World J Urol 2012;30:51–7.
[48] Koo H, Allan RN, Howlin RP, Stoodley P, Hall-Stoodley L. Targeting microbial biofilms: current and prospective therapeutic strategies. Nat Rev Microbiol 2017; 15:740–55.
[49] Fleming D, Rumbaugh KP. Approaches to dispersing medical biofilms. Microorganisms 2017;5:15.
[50] Worthington RJ, Richards JJ, Melander C. Small molecule control of bacterial biofilms. Org Biomol Chem 2012;10:7457–74.
[51] Reza A, Sutton JM, Rahman KM. Effectiveness of efflux pump inhibitors as biofilm disruptors and resistance breakers in gram-negative (ESKAPEE) bacteria. Antibiotics 2019;8:229.
[52] Vestby LK, Gronseth T, Simm R, Nesse LL. Bacterial biofilm and its role in the pathogenesis of disease. Antibiotics 2020;9:59.
[53] Bazaka K, Jacob MV, Crawford RJ, Ivanova EP. Efficient surface modification of biomaterial to prevent biofilm formation and the attachment of microorganisms. Appl Microbiol Biotechnol 2012;95:299–311.
[54] Qvortrup K, Hultqvist LD, Nilsson M, et al. Small molecule anti-biofilm agents developed on the basis of mechanistic understanding of biofilm formation. Front Chem 2019;7:742.
[55] Rabin N, Zheng Y, Opoku-Temeng C, Du Y, Bonsu E, Sintim HO. Agents that inhibit bacterial biofilm formation. Future Med Chem 2015;7:647–71.
[56] Chung PY, Khanum R. Antimicrobial peptides as potential anti-biofilm agents against multidrug-resistant bacteria. J Microbiol Immunol Infect 2017;50: 405–10.